LA-UR- 09-04889

Approved for public release;
distribution is unlimited.

Title:	Shock Initiation Behavior of PBXN-9 Determined by Gas Gun Experiments
Author(s):	Nathaniel J. Sanchez Richard L. Gustavsen Daniel E. Hooks
Intended for:	APS

Form 836 (7/06)

Shock Initiation Behavior of PBXN-9 Determined by Gas Gun Experiments

N. J. Sanchez, R. L. Gustavsen & D. E. Hooks

Los Alamos National Laboratory, Los Alamos NM 87545

Abstract. The shock to detonation transition was evaluated in the HMX based explosive PBXN-9 by a series of light-gas gun experiments. PBXN-9 consists of 92 wt% HMX, 2wt% Hycar 4054 & 6 wt% dioctyl adipate with a density of 1.75 g/cm³ and 0.8% voids. The experiments were designed to understand the specifics of wave evolution and the run distance to detonation as a function of input shock pressure. These experiments were conducted on gas guns in order to vary the input shock pressure accurately. The primary diagnostics were embedded magnetic gauges, which are based on Faraday's law of induction, and Photon Doppler Velocimetry (PDV). The run distance to detonation vs. shock pressure, or "Pop plot," was redefined as $\log(X^*) = 2.14\text{-}1.82 \log(P)$, which is substantially different than previous data. The Hugoniot was refined as $U_s = 2.32 + 2.21U_p$. This data will be useful for the development of predictive models for the safety and performance of PBXN-9 along with providing increased understanding of HMX based explosives in varying formulations.

Keywords: Plastic Bonded Explosives, HMX, Shock Initiation, Hugoniot.
PACS: 82.40.Fp. 62.50.Ef

INTRODUCTION

Shock initiation work on PBXN-9 (once designated as PBXW-9 Type II) prior to this study concluded that PBXN-9 was less sensitive than typical HMX based explosives. Results from large-scale gap tests indicate PBXN-9 to be less sensitive than Comp-B while small-scale gap tests indicated sensitivity similar to Comp-B [1]. The 50% detonation gap width for the Naval Surface Warfare Center (NSWC) large-scale gap tests ranged between 45 and 52 mm. Run distance to detonation vs. shock pressure tests conducted by Schilling and Martin produced data similar to Comp-B [2].

EXPERIMENTAL PROCEDURE

A light gas gun was used to impart a planar shock wave on a target of PBXN-9; three single stage and two two-stage gas gun experiments were performed. The gas gun minimizes tilt and structure in the imparted shock, reducing overall error in the measurement. The details and implementation of this kind of experiment are described in detail by Sheffield et al [3]. A projectile is faced with an impactor that is flat within 4μm across the central 80%. The single-stage impactors used in these experiments were z-cut quartz and z-cut sapphire while the two-stage impactors were Kel-F 81 (3M). The PBXN-9 was provided in a machined state from the Redstone Arsenal in Huntsville, AL. The samples were 50.8 mm in diameter by 25 mm thick. The immersion density of each piece of PBXN-9 was measured by and ranged from 1.756 to 1.760 g/cc.

When the impactor strikes the explosive sample a planar shock wave is generated which begins the initiation process. Electromagnetic particle velocity gauges are embedded at 9 different depths. Additionally, there are three "shock tracker"

elements, which are simply short wire segments with a regular period that can be used to measure the position of the shock front. These gauges are based on Faraday's law of induction. For a conductor of length L moving with velocity u in a steady uniform magnetic field of strength B, the induced voltage in the conductor is, $V = L \cdot u \times B$. All quantities in the equation except voltage are vector quantities. However, if by design all vectors are mutually orthogonal, this reduces to the scalar equation, $V = LuB$. B and L are measured prior to the experiment and V is recorded as a function of time during the experiment. As the conductor moves with the material, u is the particle velocity of the material at the particular LaGrangian position of the gauge.

Wave profiles of particle velocity vs. time were obtained for five experiments with input pressures of 3.33, 4.02, 5.06, 6.7 and 7.72 GPa. Input pressures were computed using the impedance matching technique [4]. Hugoniot data for these calculations was from Sheffield et al for Kel-F 81, [5] Knudsen for z-quartz, [6] and Barker and Hollenbach for z-sapphire [7]. For the initial calculation, the Hugoniot for PBXN-9 was $U_s = 2.27 + 2.07\, u_p$ which is a fit obtained using the data of Dick and Martinez [8] and Schilling and Martin [2]. Ultimately, however, the pressure reported was recalculated using the refined Hugoniot of $U_s = 2.32 + 2.21\, u_p$ by using all of the Hugoniot data from the experiments conducted here.

The method for obtaining x* & t* coordinates is outlined by Hill & Gustavsen [9]. The data gathered is fit to a second order differential equation which mimics the shock front behavior.

$$\ddot{x} = \frac{\left(\frac{a}{100}\right)\dot{x}^{b+2}(\dot{x}-C)^{b+1}(D_{CJ}-\dot{x})}{(2\dot{x}-C)(D_{CJ}-0.99\dot{x})} \qquad (1)$$

In Eq. 5 the a parameter controls the initial acceleration of the wave while the b parameter controls where turnover to detonation occurs. C = 2.32 km/s is the intercept of the Hugoniot in the shock velocity - particle velocity plane. D is the Chapman Jouguet detonation velocity. The equation is solved numerically for $x(t)$ for the point of maximum curvature, giving an accurate measure of run distance to within +/- 0.4 mm. The method for determining Hugoniot points from the data is outlined in detail by Gustavsen et al [10].

RESULTS AND DISCUSSION

Tables 1 & 2 summarize the experimental results obtained in addition to those of Schilling & Martin. Figures 1 & 2 show particle velocity and shock tracker data reduced to position and time with fits and residuals to determine the shock and detonation velocities are shown for shot 1s-1413. The resulting Pop plot and Hugoniot are shown in Figures 3 and 4, respectively. Similar data was obtained for all five shots.

Table 1.

Shot #	Density (g/cc)	Impact Vel. (km/s)	Impactor	Impact P (GPa)	Distance to Det. (mm)	Time to Det. (micro s)
1s-1386	1.757	0.727	z-sapphire	4.02	10.6	2.57
1s-1387	1.759	0.745	z-quartz	3.33	16.2	4.16
1s-1413	1.755	0.844	z-sapphire	5.06	7.47	1.69
2s-351	1.757	1.981	kel-F 81	7.72	3.4	0.66
2s-400	1.756	1.787	kel-F 81	6.7	4.16	0.89
NWC [2]	1.73			12.7	2.8	0.27
NWC [2]	1.73			8.28	5.5	0.7
NWC [2]	1.73			4.23	13	1.9
NWC [2]	1.73			2.86	19	2.5

Table 2. Particle velocity (u_p) and shock velocity (U_s) data reduced from three experiments along with data from reference 2.

Shot #	U_p	U_s	Shot #	U_p	U_s
1s-1387	0.534	3.279	1s-1386	0.614	3.545
	0.618	3.719		0.794	4.374
	0.613	3.801		0.94	4.645
	0.638	3.897		1.199	5.119
	0.643	4.014	2s-351	0.98	3.981
	0.694	4.148		1.016	4.035
	0.745	4.314		1.029	4.486
	0.868	4.537		1.19	5.112
	1.082	4.868		1.625	6.181
	1.553	5.456	NWC[2]	1.38	5.2
NWC[2]	0.549	3.01	NWC[2]	1.09	4.39
			NWC[2]	0.632	3.87

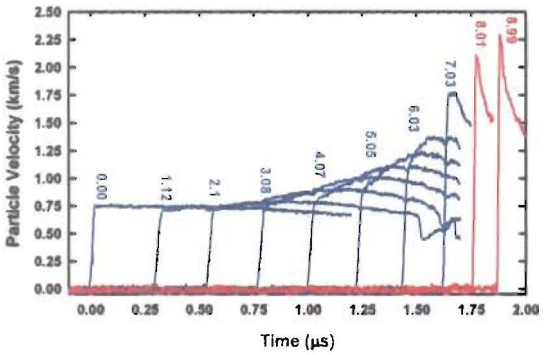

Figure 1. Data from shot number 1s-1413, sapphire impactor and input pressure of 5.06 GPa. The particle velocity gauge records are shown with particle velocity as a function of time; the gauge depths in mm are shown. Red traces indicate detonation.

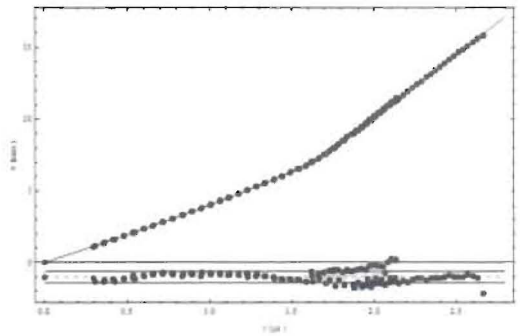

Figure 2. Reduced shock tracker data with points plotted in distance versus time with linear fits for shock and detonation velocity. Residuals are shown beneath the plot.

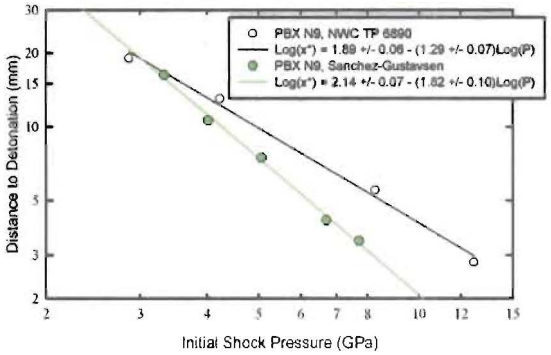

Figure 3. Pop plot showing the five current experiments along with results in reference 2. Fits to the data with parameters are given in the legend.

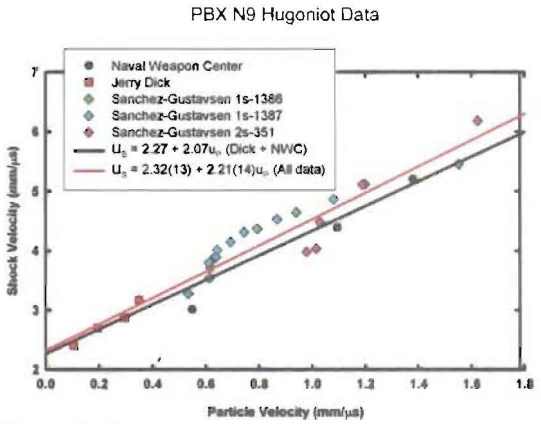

Figure 4. Hugoniot data reduced from the three current experiments plotted with all available previous data. Fits and parameters are given in the legend.

CONCLUSIONS

While the run distance at low pressure agrees with previous data, there is considerable divergence at high pressure. In fact, while the previous data was consistent with the Pop plot of Comp B, the new data is consistent with most other HMX based explosives in showing shorter run distances than Comp B at higher pressures. The difference in data might be attributed to two of the features of the previous experiments. First, the "mouse trap" configuration used to generate the plane wave is known for generating only rough planarity [11]. Second, the camera arrangement employed a large angle between camera and wedge face. These details in the experiment contributed to significant errors with respect to the breakout time measurements on the x(*t) plots, This makes it difficult to determine where detonation begins in contrast to figure 2 of this work.

ACKNOWLEDGEMENTS

This research was funded by the Joint DoD/DOE Munitions Technology Development Program. Special Thanks to Lee Gibson & Brian Bartram for firing these shots.

REFERENCES

1. B. Baulder, R. Hutcheson, M. Gallant, and J. Leahy, Characterization of PBXW-9, Naval Surface Warfare Center Report NSWC TR 86-334, Dahlgren, VA and Silver Spring, MD (August 1989).
2. T. Schilling and S. Martin, Shock Sensitivity and Wedge Testing of PBXW-9, Naval Weapons Center Report NWC TM 6890, China Lake, CA, (March 1988).
3. S. A. Sheffield, R.L. Gustavsen, and R.R. Alcon, In-situ Magnetic Gauging Technique Used at LANL-Method and Shock Information Obtained, in *Shock Compression of Condensed Matter- 1999*, M. D. Furnish, L. C. Chhabildas, and R. S. Hixson, Eds., (AIP Conference Proceedings, Melville, NY), (2000).
4. R. G. McQueen, S. P. Marsh, J. W. Taylor, J. N. Fritz, and W. J. Carter, *High Velocity Impact Phenomena*, (Academic Press, New York, NY), (1970).
5. S. A. Sheffield and R. R. Alcon, In-situ Magnetic Gauge Measurements in Kel-F, in *Shock Compression of Condensed Matter-1991*, S. C. Schmidt, R. D. Dick, J. W. Forbes, and D. G. Tasker, Eds., (North-Holland, Amsterdam, The Netherlands), 909, (1992).
6. M. D. Knudsen, "Use of Pico-Second Electronic Spectroscopy to Understand Phase Transitions in Shocked Cadmium Sulfide," Ph. D. Thesis, Washington State University, Pullman, WA, (1998).
7. L. M. Barker, and R. E. Hollenbach, Shock-Wave Studies of PMMA, Fused Silica, and Sapphire, J. Appl. Phys.**41(10)**, 4208 (1970).
8. J. J. Dick and A. R. Martinez, "Plane Impact Experiments on PBX 9501 and PBXN-9," in *The Joint DoD/DOE Munitions Technology Development Program Progress Report for FY97*, Los Alamos National Laboratory Technical Report LA-13415-PR, Joe V. Repa, Ed., Los Alamos, NM (August 1998), pages 38-40.
9. L. G. Hill and R. L. Gustavsen, On the Characterization and Mechanisms of Shock Initiation in Heterogeneous Explosives, in *12th International Detonation Symposium*, (Office of Naval Research, Arlington, VA), 975, (2003).
10. R. L. Gustavsen, S.A. Sheffield, and R.R. Alcon, Measurements of Shock Initiation in the Tri-amino-tri-nitro-benzene Based Explosive PBX 9502: Wave Forms From Embedded Gauges and Comparison of Four Different Material Lots, J. Appl. Phys. **99(11)**, 114907 (2006).
11. A. K. Hopkins, P. C. Chou, *Dynamic Response of Materials to Intense Impulsive Loading*, (Air Force Materials Lab, Wright-Patterson AFB, OH), 1972.